Photodestruction spectroscopy of carbon disulfide cluster anions (CS2)-n, n = 1-4: Evidence for the dimer core structure and competitive reactions of the dimer anion

doi: 10.1063/1.475510

Photodestruction spectroscopy of carbon disulfide cluster anions $(CS_2)_n^-$, $n=1-4$: Evidence for the dimer core structure and competitive reactions of the dimer anion

Toshihiko Maeyama, Takanobu Oikawa, Tohru Tsumura, and Naohiko Mikami[a)]
Department of Chemistry, Graduate School of Science, Tohoku University, Aoba-ku, Sendai 980-77, Japan

(Received 9 September 1997; accepted 16 October 1997)

Photodestruction spectra of carbon disulfide cluster anions, $(CS_2)_n^-$, $n=1-4$, have been measured with a time-of-flight mass spectrometer coupled with an optical parametric oscillator. The spectra of all the cluster anions of $n\geqslant 2$ were found to exhibit a similar absorption band peaking at 1.6–1.8 eV, suggesting that a $C_2S_4^-$ core is involved in the cluster anions. Photon energy dependence of competition between electron detachment and dissociation of the dimer anion was also observed. It was found that there is a reaction channel of the dimer anion producing $C_2S_2^-$ and S_2, as well as the ordinary dissociation into CS_2^- and CS_2. The most stable form of the dimer anion was investigated by *ab initio* calculations at the unrestricted Hartree–Fock/6-31+G* level, showing that the stable form involves covalent C–C and S–S bonds. Reaction mechanisms are discussed on the basis of electronic symmetries of the parent and the fragments. © *1998 American Institute of Physics.* [S0021-9606(98)01804-2]

I. INTRODUCTION

Recent experiments on the photoelectron spectroscopy[1] of molecular cluster anions have shown that the binding energy of an excess electron is generally a few electron volts. It is comparable with intermolecular binding energies for their cluster formation, so that electron detachment and dissociation may compete in photodestruction processes of cluster anions. This is the similar situation encountered in ''super-excited'' states[2] of neutral molecules which may decay through ionization and dissociation. Moreover, excitation energy of competitive destruction for anions is considerably lower than that for the neutrals, i.e., the process for anions may occur in the near-infrared to visible region. Since decay dynamics of cluster anions near detachment threshold is closely related to their electronic structure, spectroscopy in the near-infrared region is quite interesting with respect to the mechanism of reactions induced by electron transfer.

Carbon disulfide (CS_2) is one of the most reactive electrophilic reagents, which is frequently used as a medium for organic syntheses. It has been also reported that it polymerizes[3,4] under high-pressure conditions or in discharge circumstances. Spectroscopic analyses on the reactivity and structure of cluster anions $(CS_2)_n^-$ may be a keystone by which to elucidate reaction mechanisms under bulk conditions. Nevertheless, photodestruction processes have never been reported for $(CS_2)_n^-$, although there have been many reports for the neutral and the positive ion clusters. For example, Ng and co-workers[5,6] have carried out extensive studies on ionization and/or dissociation channels of CS_2 clusters following photoexcitation with a continuous vacuum ultraviolet (VUV) light source. To our knowledge, there are only two experiments published for $(CS_2)_n^-$, i.e., generation by Rydberg electron attachment[7] and measurement of thermochemical functions[8] using a high-pressure mass spectrometer. Very recently, Nagata and co-workers[9] observed photoelectron spectra of $(CS_2)_n^-$.

Another important aspect also is that CS_2 is an ''isovalent'' molecule of CO_2. Both molecules are well known to be linear in their neutral ground state. Hence, a comparison between results for CS_2 and CO_2 cluster anions provides us with much of chemical interest. Fleischman and Jordan[10] have calculated stable geometries of the CO_2 dimer anion, where there can be two isomers, which are almost isoenergetic, the equivalent form (D_{2d} symmetry) and the ion–molecule complex form (C_s symmetry). Johnson and co-workers[11] have reported the photoelectron spectra of $(CO_2)_n^-$ for $n=2-13$, suggesting the presence of isomers. Their data suggested that the dimer core structure is predominant for $n\leqslant 5$, and that the monomer core structure is more stable for $n\geqslant 6$. Lineberger and co-workers[12] have reported photodissociation of much larger cluster anions ($13\leqslant n\leqslant 40$), where they have noted that electron detachment is the only photodestruction channel for $n\leqslant 12$.

In the present work, we report photodestruction spectra of $(CS_2)_n^-$, $n=1-4$. We have observed the photon energy dependence of the destruction channels for the dimer anion, where electron detachment and two dissociation channels are found to compete with each other. In addition to the ordinary dissociation channel leading to CS_2^- and CS_2, we have found another channel generating intracluster reaction products of $C_2S_2^-$ and S_2. *Ab initio* calculations at the unrestricted Hartree–Fock level with the 6-31+G* basis set have been performed for the monomer and the dimer systems. Structures and reaction mechanisms of the dimer anion are discussed in comparison with the calculated results.

a)Author to whom correspondence should be addressed; electronic mail: mae@qclhp.chem.tohoku.ac.jp

 0021-9606/98/108(4)/1368/9/$15.00

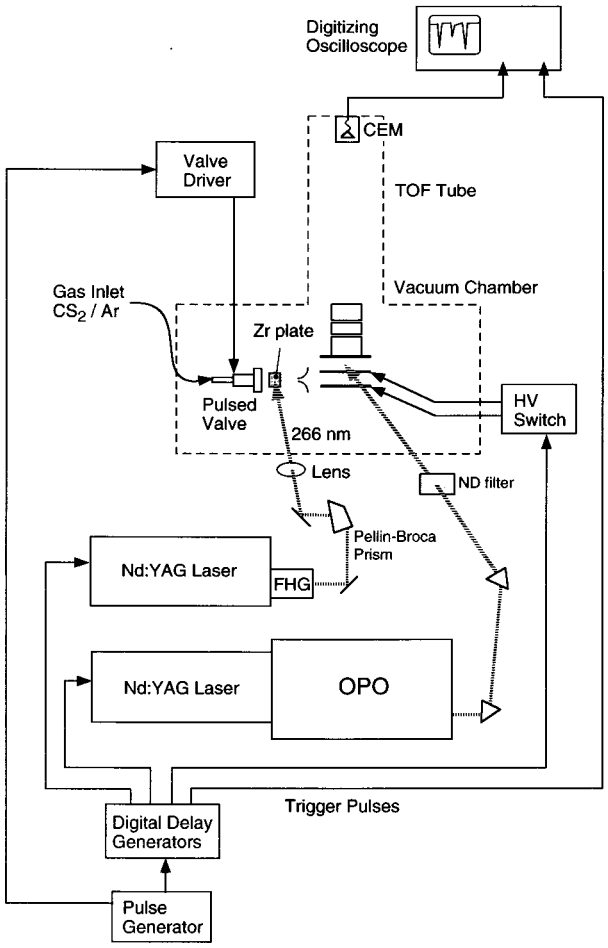

FIG. 1. Schematic of the experimental setup for photodestruction spectroscopy of cluster anions.

II. EXPERIMENT

The experimental apparatus and the procedures were mostly identical to those described elsewhere.[13] Figure 1 shows a schematic of the experimental setup.

A gaseous mixture of CS_2 and Ar was supersonically expanded as a free jet into a vacuum chamber through a pulsed valve (General Valve Co.) with a 0.5 mm orifice. The partial vapor pressure of CS_2 was about 200 Torr and the total stagnation pressure was 4 atm. A zirconium metal plate was located on one side of the valve 15 mm from the axis of the beam. The fourth harmonic of a Nd:YAG laser (Spectra Physics GCR230) was introduced to hit the zirconium surface after a certain time delay from opening of the valve. The pulse energy of the incident laser light was typically 20 mJ. It was loosely focused so that the spot diameter on the surface was about 3 mm. Cluster anions were generated by attachment of photoejected electrons from the metal surface to the neutral CS_2 clusters in the expansion region of the jet. A similar electron attachment technique, using a Y_2O_3 disk as an electron source, was developed by Nakajima *et al.*[14] The jet was skimmed into an ion beam by a 3 mm skimmer. The cluster anions were analyzed by using a pulsed time-of-flight (TOF) mass spectrometer of the standard Wiley–McLaren type. The pulsed voltages, the duration of which was 10 μs, were typically -1020 and -940 V for the first and the second electrodes, respectively. The ion signals were detected with a channel electron multiplier (Murata Ceratron E) and were monitored with a digitizing oscilloscope (Tektronix TDS520A).

Signal or idler outputs of an optical parametric oscillator (OPO) (Spectra Physics MOPO 730) pumped by another Nd:YAG laser (Spectra Physics GCR250) were used for the photodestruction light source. The OPO beam was collimated by irises to 1 cm in diameter and was not focused, so that the beam diameter completely covers a cross section of an ion cloud of a particular species. The fluence of the light pulse was attenuated to ~ 12 mJ/cm^2 by neutral density filters. The light pulse was introduced into the second acceleration region of the TOF spectrometer to excite a single species. Depletion of the parent ion signals was observed when photodestruction takes place.

The total photodestruction cross section[15] is given as follows:

$$\sigma_{\mathrm{tot}}(\lambda) = \xi \frac{\ln(I_0/I)}{\tau \Phi(\lambda)}, \tag{1}$$

where I and I_0 represent the numbers of parent ions at a given wavelength λ during the OPO-on and -off periods, respectively. $\Phi(\lambda)$ and τ are the photon flux and the temporal duration of the OPO light pulse, respectively. The symbol ξ is an instrumental parameter, which is unknown in this work. In this respect, we obtained photodestruction spectra by using the relative cross section,

$$\sigma'_{\mathrm{tot}}(\lambda) = \frac{\ln(I_0/I)}{\lambda \cdot \varphi(\lambda)}, \tag{2}$$

where $\varphi(\lambda)$ is the fluence of the OPO light pulse. The photodestruction spectrum corresponds to the absorption spectrum, when we assume that photoexcited anions must decay through the electron detachment and/or dissociation processes.

In this experiment, we observed a remarkable depletion of a negative ion in an energy region where photodetachment is the only destruction process of the ion. However, when dissociation channels are opened, fragment ions appear as a broad band in the lower mass number region of the parent ion in the TOF mass spectra. The fragment ions reach the ion detector faster than the parent, because the fragments are accelerated more in the electrostatic field of the photon-interaction region. Thus, we obtain the total dissociation yield of the parent ion by integrating all the fragment signals, although the species of the fragments are not identified. Comparing the total dissociation yield with the total destruction cross section, the electron detachment yield can be extracted.

III. RESULTS AND DISCUSSION

A. Photodestruction spectra of $(CS_2)_n^-$

Figure 2 shows mass spectra of the CS_2 cluster anions obtained under the OPO-off and -on conditions, where the

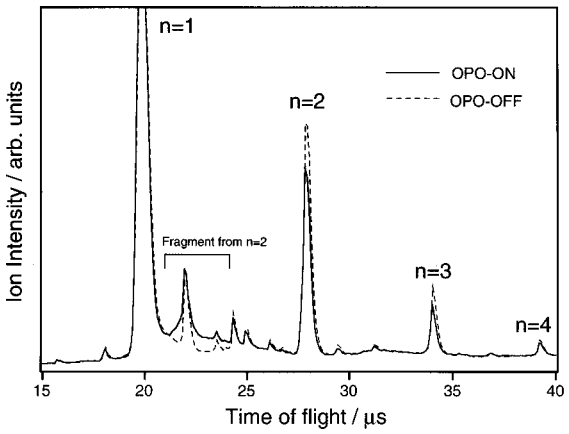

FIG. 2. Time-of-flight mass spectra of $(CS_2)_n^-$ under OPO-off (broken line) and OPO-on ($E=1.64$ eV; solid line) conditions. The input timing is tuned to excite $n=2$. Shaded regions indicate the depletion of the parent and the generation of the dissociation products.

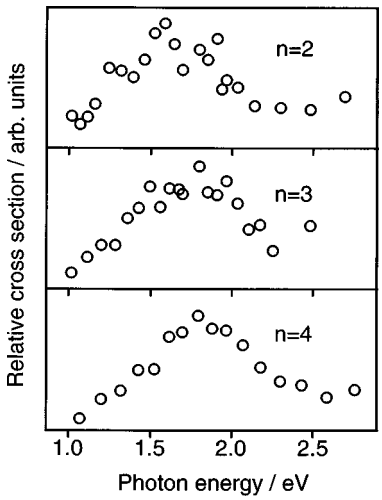

FIG. 4. Photodestruction spectra of $(CS_2)_n^-$ ($n=2-4$).

timing of the OPO light pulse irradiation was tuned to excite the dimer anion ($n=2$) and the photon energy of the OPO light was 1.64 eV. It is evident that a reduction of the parent ion signals is induced by their photodestruction, and a broad enhancement due to the fragment ions appears in the mass region between $n=1$ and $n=2$.

Figures 3 and 4 show the relative photodestruction cross sections for $n=1-4$ through Eq. (2). The spectrum of the monomer anion, CS_2^-, represents a gradual increase with respect to the photon energy. In this energy region, no dissociation process is observed, so that CS_2^- decays only by electron detachment. In this respect, this spectrum can be compared with the photoelectron spectrum of CS_2^-. Oakes and Ellison[16] measured the photoelectron spectrum of CS_2^-, where a long progression of the bending vibration appears because CS_2^- has a bent structure, whereas the neutral is linear. They determined the adiabatic electron detachment energy of CS_2^- to be 0.895 ± 0.020 eV. The extremely broad feature of the present spectrum can be understood in a similar manner; the increase of accessible vibrational states of the neutral CS_2 leads to a gradual rise of the photodetachment cross section.

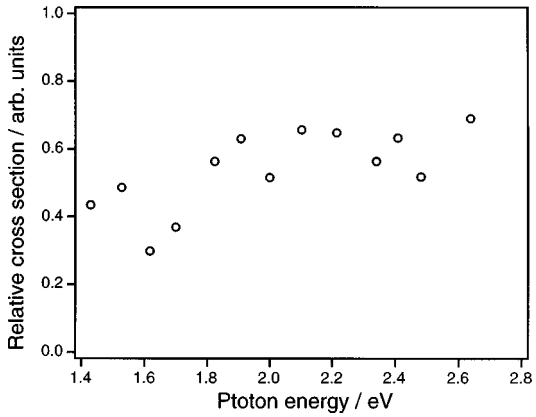

FIG. 3. Photodestruction spectrum of CS_2^-.

Photodestruction spectra of $n=2-4$ are shown in Fig. 4, and exhibit a broad absorption band peaking at 1.6–1.8 eV. The peak position seems to shift gradually to the high energy side as the cluster size increases. The onset of the absorption of $n=2$ is found at 0.9 ± 0.1 eV, which is considered to be the adiabatic transition energy from the ground state to the first excited state. The total destruction cross section for $n=2$ at the absorption peak was estimated to be 3–4 times larger than that for $n=1$ by measuring the dependence of the ion depletion ratio with respect to the OPO fluence. The larger cross sections were also observed for $n\geqslant3$. The similar spectra for $n=2-4$ suggest that the cluster anions of $n\geqslant3$ consist of a dimer anion and the neutral CS_2 moiety, which is loosely bound to the former. The dimer core anion acts as a chromophore of the similar spectra. This is consistent with thermochemical measurements by Hiraoka and co-workers,[8] where they found that the enthalpy change for clustering of CS_2^- with CS_2 ($\Delta H=-21.9$ kcal/mol) is much larger than that of the dimer anion and CS_2 ($\Delta H=-6.4$ kcal/mol). In this respect, hereafter, we represent the dimer core anion as $C_2S_4^-$ instead of $(CS_2)_2^-$.

There have been reports of several cluster ions of homogeneous species having the dimer core structure, for example, the benzene cluster cation,[17,18] $(SO_2)_n^-$,[19,20] $(CO_2)_n^-$,[11] and so on. A dimer core ion often exhibitds an absorption band with a large cross section in the near-infrared or the visible region. Such an absorption is usually assigned to the charge resonance (CR) type transition[21] between two states which arises from the $+/-$ combination of wave functions involving the neutral and the ionic configurations of two identical molecules. However, the absorption bands observed for the CS_2 cluster anions cannot be assigned to the CR type. The reason for this will be discussed in following.

B. Photodestruction channels of the dimer anion

Since the dimer anion is a key species among the small size cluster anions of CS_2, we concentrate our discussions on

the results of the dimer anion. In the photodestruction spectrum of the dimer anion, any processes leading to the disappearance of the dimer anion can contribute to the overall cross section of the spectrum. We refer to σ_{tot} as the total photodestruction cross section for the dimer anion. One of the destruction channels is the electron detachment process

$$C_2S_4^- + h\nu \rightarrow (CS_2)_2 + e^-. \tag{3}$$

Since we did not know whether the neutral species dissociates or not in the present experiment, the electron detachment means all the electron releasing processes irrespective of the dissociation in the neutral manifold. The partial cross section of reaction (3) is represented as $\sigma(e^-)$, whatever neutral fragmentation is involved. The other channel is due to dissociation processes of ionic manifold but not to the electron release. Since multiple dissociation processes are expected, the partial cross section involving all the dissociation processes is denoted as σ_{diss}. Therefore, the total cross section σ_{tot} of the photodestruction process is represented as follows:

$$\sigma_{\mathrm{tot}} = \sigma(e^-) + \sigma_{\mathrm{diss}}. \tag{4}$$

Among the dissociation channels one is due to the dissociation of the dimer anion into the neutral monomer and its anion

$$C_2S_4^- + h\nu \rightarrow CS_2^- + CS_2. \tag{5}$$

We refer to (5) as the CS_2^- channel whose partial cross section is represented by $\sigma(CS_2^-)$. The other dissociation channel will be given later.

In Eq. (4), we may define the dissociation yield, as given by

$$P_d = \sigma_{\mathrm{diss}}/\sigma_{\mathrm{tot}}, \tag{6}$$

while the yield of the electron detachment is given by

$$P_e = 1 - P_d. \tag{7}$$

P_d is obtained by measuring the intensity ratio of the fragment ion signal versus the depletion signal of the parent ion, assuming that the detection efficiencies of both ions are the same. Although the absolute value of P_d is hardly obtained, it can be revealed how P_d depends relatively on the photon energy (E). Figure 5 shows relative values of P_d as a function of E, in which we assume $P_d = 1$ at $E = 1.13$ eV. Bowen and co-workers[22] measured the photoelectron spectrum of the dimer anion, where the adiabatic electron affinity of the neutral dimer was determined to be 1.071 ± 0.032 eV. Thus, $\sigma(e^-)$ is considered to be negligibly small at $E = 1.13$ eV. Since P_d declines monotonically with an increase of the photon energy, the yield of electron detachment increases conversely. The total photodestruction cross section reaches the bottom at a photon energy around 2.3 eV, so that the direct electron detachment is considered to be the predominant channel in the energy region above this. A similar behavior has been found for $(SO_2)_2^-$, as reported by Dresch *et al.*[23]

It is quite interesting to investigate whether there are any other dissociation processes than the CS_2^- channel. Figure 6 shows an example of TOF mass spectra obtained under a condition that the cluster formation for $n \geqslant 3$ was minimized by adjusting the time duration as well as the stagnation pressure of the pulsed jet expansion. A new product band was found at $M = 88$ amu corresponding to $C_2S_2^-$ when the OPO light was introduced into the first acceleration region of the TOF spectrometer. Thus, the second dissociation channel is suggested to be as follows:

$$C_2S_4^- + h\nu \rightarrow C_2S_2^- + S_2, \tag{8}$$

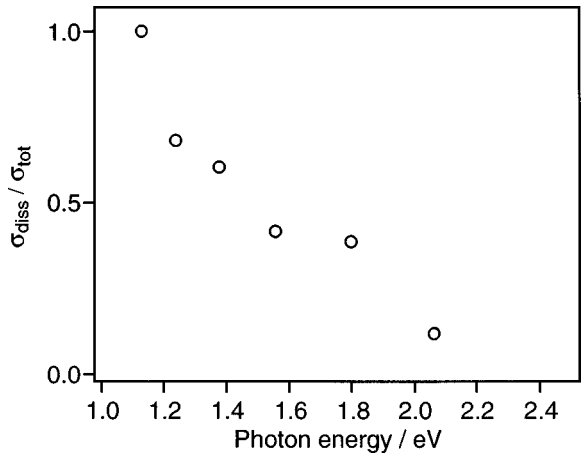

FIG. 5. Photon energy dependence of the dissociation yield with respect to the total destruction cross section.

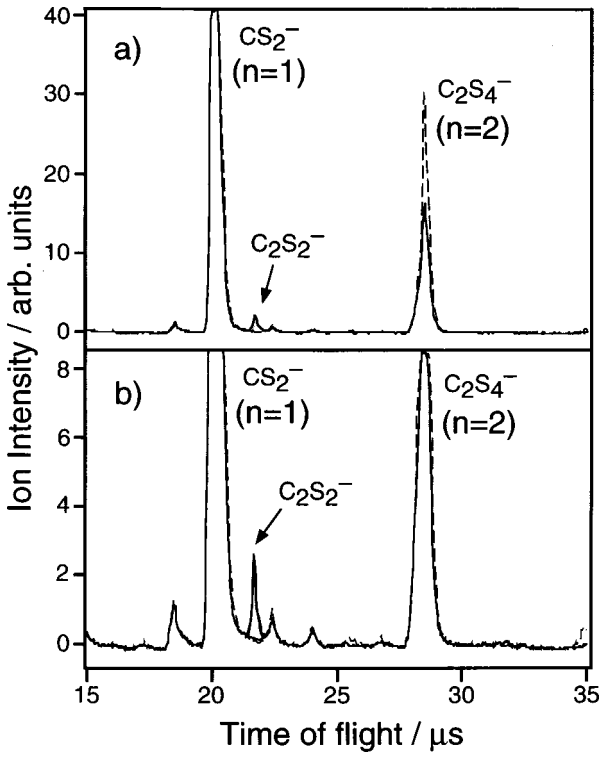

FIG. 6. (a) Time-of-flight mass spectrum where the OPO light ($E = 1.88$ eV) is introduced to the first acceleration region of the mass spectrometer (solid curve). The generation of the $n \geqslant 3$ clusters is restrained to be less than 10% of the dimer anion. The broken curve is the reference spectrum. (b) An expanded trace ($5\times$) of the upper panel. The peak corresponding to $C_2S_2^-$ appears as a dissociation product.

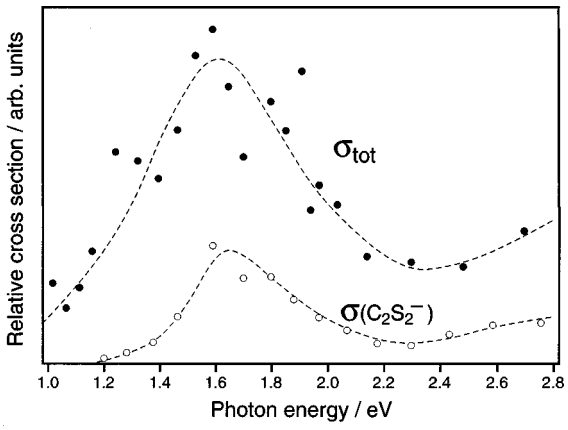

FIG. 7. The partial cross sections for the $C_2S_2^-$ channel (open circles) and the total destruction cross sections (closed circles) on a relative scale.

which we call the $C_2S_2^-$ channel. The partial cross section of this channel is given by

$$\sigma(C_2S_2^-) = \sigma_{\text{tot}} \times I(C_2S_2^-)/\Delta I(C_2S_4^-), \tag{9}$$

where $I(C_2S_2^-)$ is the signal intensity of $C_2S_2^-$, and $\Delta I(C_2S_4^-)$ is the depletion of the parent dimer ions. No other dissociation channel was found in any energy region of our measurements. Thus, σ_{diss} is expected to be as follows:

$$\sigma_{\text{diss}} = \sigma(CS_2^-) + \sigma(C_2S_2^-). \tag{10}$$

The photon energy dependence of $\sigma(C_2S_2^-)$ is shown in Fig. 7. The onset of the $C_2S_2^-$ generation occurs at 1.2 eV, although σ_{tot} at the same energy is almost half of the peak value. Therefore, the CS_2^- channel should be predominant in the photodestruction threshold at around 1 eV, since no electron detachment takes place in this region, as discussed above. Unfortunately, the branching ratios of each dissociation channel were not determined with our experiments, because $I(C_2S_2^-)/\Delta I(C_2S_4^-)$ in Eq. (9) must be multiplied by a constant but unknown factor corresponding to the ion detection efficiency. Despite this, it should be noted that $\sigma(C_2S_2^-)$ does not disappear even at 2.3 eV, where the absorption cross section is minimal. Hence, we presume that the $C_2S_2^-$ channel is dominant over the CS_2^- channel in the energy region higher than 2.0 eV.

C. Hartree–Fock calculations for the dimer anion

Since the broad and structureless feature of the photodestruction spectrum is not effective for determining the geometric structure of the cluster anion, *ab initio* calculations provide valuable clues to the relation between the structure and the reaction mechanism. Hiraoka and co-workers[8] calculated the geometry and the energy of the stable dimer anion at the restricted open-shell Hartree–Fock (ROHF) level with the 6-31G basis set. They showed that the most stable form of $C_2S_4^-$ is of C_{2v} symmetry where the symmetric axis is perpendicular to the C–C axis. However, the 6–31G basis set is insufficient for negatively charged systems to be calculated, since the diffuse wave function of the excess electron orbital must be involved. Besides, it is better to apply

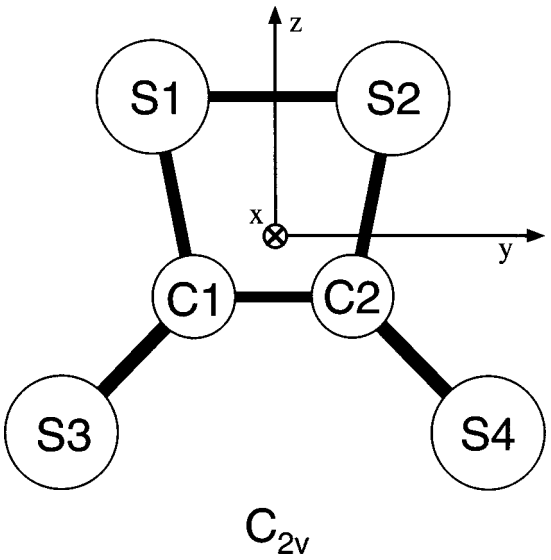

FIG. 8. The optimized geometry of the $C_2S_4^-$ anion.

the unrestricted Hartree–Fock (UHF) method for calculations of the absolute energies, although the ROHF results may provide qualitative insights such as highest occupied molecular orbital–lowest occupied molecular orbital (HOMO–LUMO) correlations. In this respect, we have calculated at the UHF/6-31+G* level for the negative ions and at the RHF/6-31+G* level for closed-shell neutral molecules, respectively. The computations were performed with the GAUSSIAN92 program package[24] on a workstation (Hewlett–Packard Apollo9000 735). More sophisticated methods, for example, the second-order Møller–Plesset (MP2) perturbation theory, have never been feasible in our computational environment to calculate systems including heavy atoms like sulfur, unfortunately.[25] Freischman and Jordan[10] reported that the most stable isomer of the CO_2 dimer anion at the UHF level is altered by the other isomer when they applied the MP2 level of theory. In the present calculations, therefore, we did not employ the MP2 calculation, although the absolute value of the calculated energies may not be very accurate.

The most stable geometry of $C_2S_4^-$ at the UHF/6-31+G* level was found to be of C_{2v} symmetry as well as at the ROHF/6-31G level, as depicted in Fig. 8. Internuclear dis-

TABLE I. Optimized parameters of $C_2S_4^-$ in the C_{2v} geometry.

Bond lengths and angles[a]	ROHF/6-31G	ROHF/6-31+G*	UHF/6-31+G*
Bond lengths (Å)			
C1-C2	1.39	1.41	1.40
C1-S1	1.87	1.79	1.79
C1-S3	1.70	1.65	1.66
S1-S2	2.26	2.09	2.09
Bond angles (deg)			
∠S1-C1-C2	103.4	101.0	101.0
∠S1-C1-S3	123.4	125.5	125.3

[a]The number given to each atom is identical with that in Fig. 8.

TABLE II. Mulliken charge and spin densities for $C_2S_4^-$ in the optimized geometries.

	ROHF/6-31G		ROHF/6-31+G*		UHF/6-31+G*	
	Charge	Spin	Charge	Spin	Charge	Spin
C1	−0.488	0.186	+0.081	0.190	+0.056	0.000
S1	0.102	0.015	−0.033	0.028	−0.042	0.001
S3	−0.114	0.298	−0.548	0.281	−0.514	0.496

tances and bond angles obtained at three different levels are summarized in Table I. Close distances of C1–C2 and of S1–S2 suggest the covalent bond formation for both, so that the dimer anion may seem to be a so-called four-centered reaction intermediate. Especially, the bond length between these carbon atoms is comparable to that of double bonds of unsaturated hydrocarbons. Inclusion of diffuse functions in the basis set was found to be effective for the S1–S2 bond formation. The electronic ground state was found to be $^2B_1$ irrespective of the level used for the calculation. However, the electron and the spin densities on each atom depend on the level, which are summarized in Table II. The result of the UHF/6-31+G* level reveals that the excess electron localizes on sulfur atoms on the open sites, namely, S3 and S4. Hiraoka *et al.*[8] showed the optimized geometry of the trimer anion at the ROHF/6-31G level, where a neutral monomer attaches weakly to the open side of the dimer anion by an electrostatic interaction. However, it should be noted that the interaction potential between the neutral and the dimer anion is a delicate matter depending on the electron density on each atom.

Obviously, the calculated geometry of the dimer anion suggests that cleavages of the four-membered ring with respect to the **y** and to the **z** axes result in the CS_2^- and the $C_2S_2^-$ channels, respectively. The optimized geometries of the neutral and the anionic fragments are shown in Fig. 9. The electronic ground states of CS_2^-, CS_2, and S_2 are $^2A_1$, $^1\Sigma_g^+$, and $^3\Sigma_g^-$, respectively. The bent form of CS_2^- is consistent with the photoelectron spectrum, where a long progression of bending vibrations appears. On the other hand, $C_2S_2^-$ was found to be linear. The C–C bond length is so small that it corresponds to a triple bond of acetylene. It was found that the Y-shaped isomer having a form like vinylidene is unstable. It confirms that the departing S_2 molecule in the $C_2S_2^-$ channel is attributed to the form in which

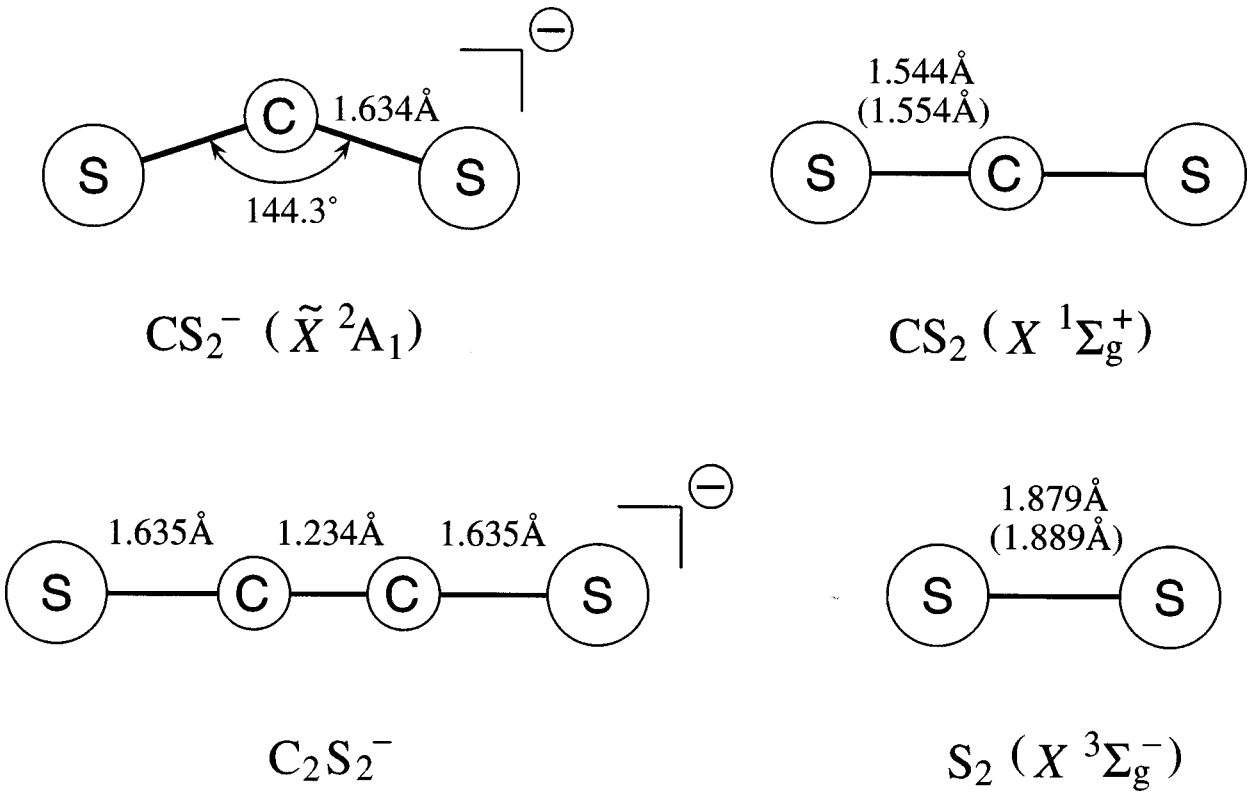

FIG. 9. The optimized geometries of the dissociation products of $C_2S_4^-$. The optimizations are performed for CS_2^- and $C_2S_2^-$ at the UHF/6-31+G* level for CS_2 at the RHF/6-31G* and for S2 at the UHF/6-31G*. Bond lengths of neutral molecules (in parentheses) are the experimental values in Refs. 27 and 28.

TABLE III. Harmonic vibrational modes of $C_2S_4^-$ in the optimized geometry at the UHF/6-31+G* level.

Mode	Symmetry	Frequency[a] (cm^{-1})	Force constant (mdyne/Å)
1	a_2	126.6	0.30
2	a_1	196.5	0.69
3	b_1	298.4	0.70
4	b_2	314.7	1.50
5	b_2	390.8	2.67
6	a_1	483.0	4.19
7	a_1	562.9	5.94
8	a_2	594.4	2.57
9	b_2	752.0	4.78
10	a_1	967.4	7.53
11	b_2	1168.9	10.37
12	a_1	1499.6	16.15

[a]No scaling factors are multiplied.

S1 and S2 are in the four-membered ring. Although electronic symmetry of the stable linear shape could not be simply determined by the calculation, A_1 symmetry has been obtained when it takes a trapezoidal (C_{2v}) shape. Electronic correlations between the parent and the fragments will be discussed in Sec. III D.

We also calculated vibrational energies of the dimer anion at the UHF/6–31+G* level. There are 12 vibrational modes which are given in Table III. Force constants of totally symmetric (a_1) modes provide useful information of bond strengths in the four-membered ring. Five a_1 modes are schematically represented in Fig. 10. Mode 12 ($1499.6\ cm^{-1}$) is assigned to the C–C stretching vibration, which is consistent with its bond length corresponding to a double bond. Mode 10 ($967.4\ cm^{-1}$) is the stretching vibration of the four-membered ring with respect to the **z** axis. Its force constant was found to be 7.53 mdyne/Å, which is substantially lower than that of mode 12 (16.15 mdyne/Å), showing that the C–S bonds in the four-membered ring are relatively loose.

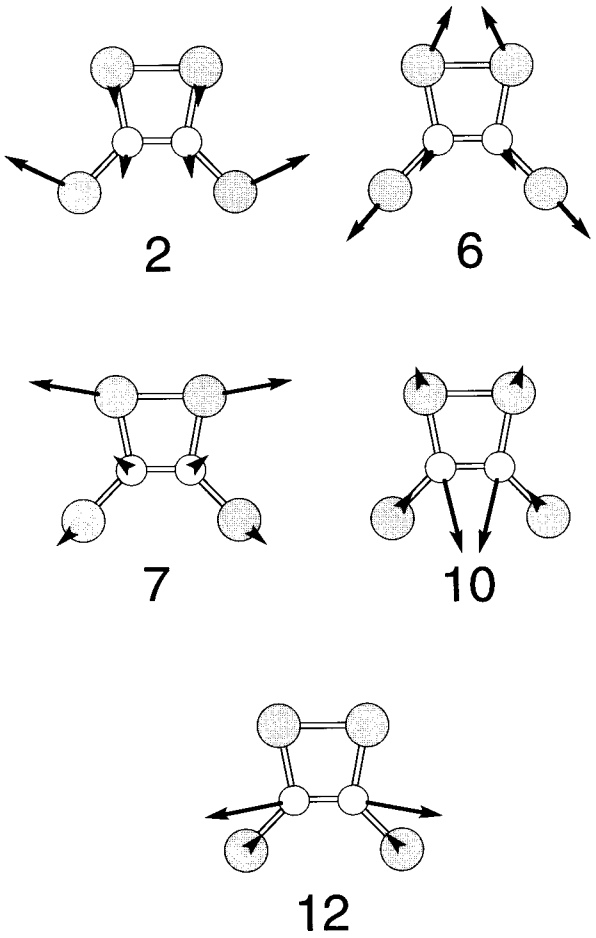

FIG. 10. Totally symmetric (a_1) vibrational modes of $C_2S_4^-$. The nuclear motions, represented by arrows, are exaggerated by multiplying a constant factor to the calculational results.

D. Reaction mechanisms of the dimer anion

Figure 11 shows a schematic diagram of potential energy surfaces (PESs) of the $C_2S_4^-$ system. Although there are some ambiguities for energy levels of the product states, Fig. 11 contains the essence of competition between the destruction channels. When the dimer anion is photoexcited, the first step of the competition occurs between the direct electron detachment and a transition to an excited state of the anion. The neutral surface drawn with a broken curve may lie near the excited state at the equilibrium geometry of the ground state anion. The second step is decay processes of the excited state, i.e., the CS_2^- channel, the $C_2S_2^-$ channel, and maybe vibrational autodetachment.

Correlations between electronic states of the parent anion and the fragments provide us with significant information about reaction mechanisms. As was discussed in Sec. III C, the competitive dissociation channels are attributed to bond cleavages of the four-membered ring with respect to two in-plane axes, namely, **y** and **z**. Note that we use the definition for axes shown in Fig. 8, even though symmetries of the fragments are concerned. The reflection symmetry of the electronic wave function must be preserved through the dissociation processes, if it proceeds without destroying the molecular plane.

The asymptotic state for the CS_2^- channel is $CS_2^-(^2A_1) + CS_2(^1\Sigma_g^+)$. The electronic wave function of the whole system is symmetric with respect to the reflection $\sigma(\mathbf{yz})$, where each atom of the fragments is located within the **yz** plane. If the dominant interaction to form the dimer anion is the CR type, the ground state of the dimer anion must correlate with the ground asymptotic state of $CS_2^- + CS_2$. However, it is readily found that the CS_2^- channel does not correlate with the ground $^2B_1$ state of $C_2S_4^-$, since the $^2B_1$ state exhibits antisymmetric behavior with respect to $\sigma(\mathbf{yz})$. Symmetries of the electronic excited states, which can be accessed through the one-photon transition from the ground $^2B_1$ state, are A_1, A_2, and B_1. Among them, only A_1 state can correlate with the CS_2^- channel, where the direction of the transition dipole moment is parallel to the out-of-plane axis **x**. Thus, we concluded that the observed absorption band with a peak of 1.6 eV is due to the $^2A_1 \leftarrow {}^2B_1$ transition. Hiraoka and co-workers[8] have suggested that there is a barrier to the

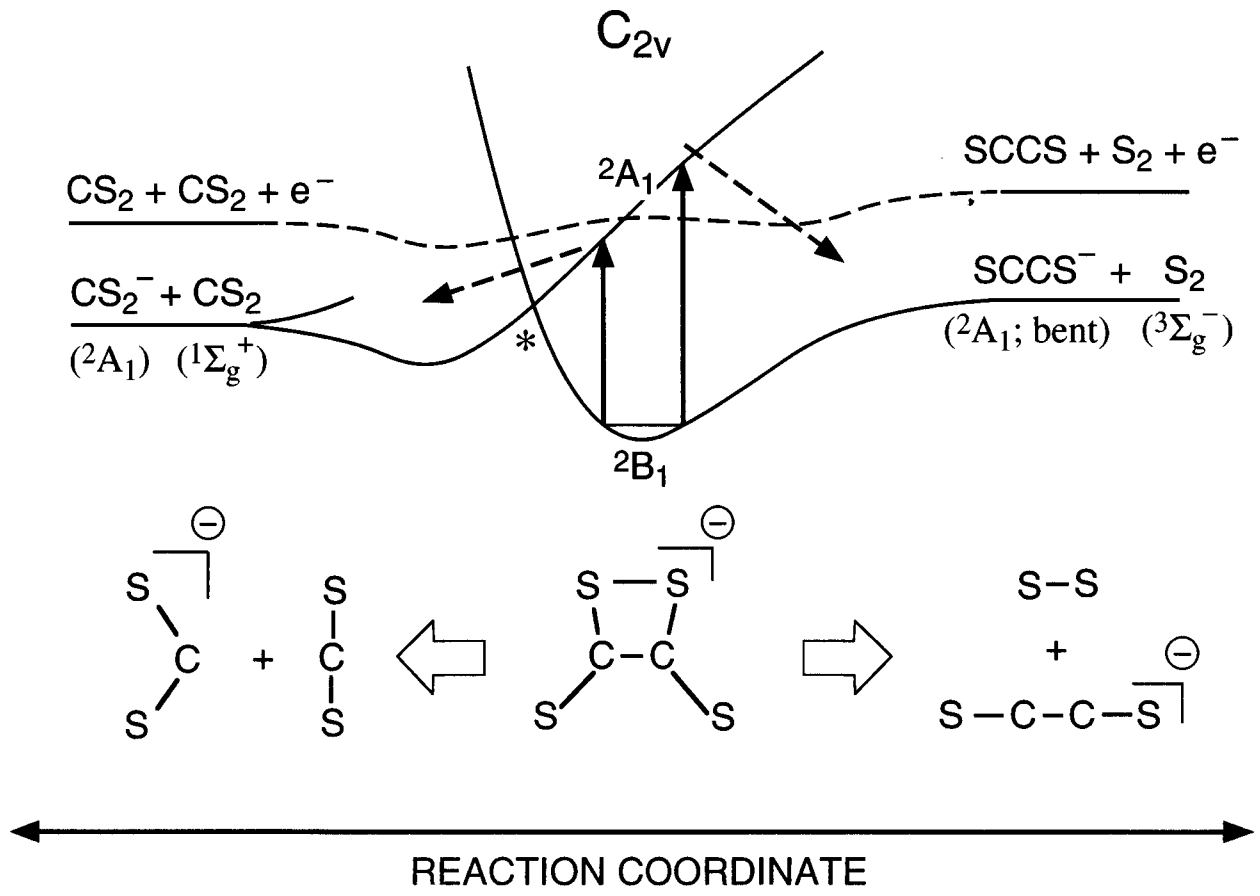

FIG. 11. Schematic potential energy surfaces for $C_2S_2^-$. Dissociation channels in the **y** and **z** directions correspond to the right-hand side and the left-hand side pathways, respectively. The broken curve represents the neutral surface where electron detachment occurs. The potential barrier suggested by Hiraoka and co-workers (Ref. 8) may be attributed to the crossing point between the $^2B_1$ and $^2A_1$ states (marked with an asterisk).

dimer anion formation from CS_2^- and CS_2. We presume that it arises as a result of a crossing between PESs of the ground $^2B_1$ and $^2A_1$ states, which is indicated by an asterisk in Fig. 11.

For the $C_2S_2^-$ channel, the asymptotic state is composed of $C_2S_2^-$ ($^2A_1$ in a C_{2v} form) and S_2 ($^3\Sigma_g^-$). Direct product between them yields the B_1 symmetry in C_{2v}, so that the $C_2S_2^-$ channel is allowed to correlate with the ground state of the dimer anion, since the ground $^3\Sigma_g^-$ state of S_2 exhibits the antisymmetric character with $\sigma(\mathbf{yz})$. Therefore, predissociation following internal conversion from the $^2A_1$ state to the ground state is most likely for the channel. The C–S bonds in the four-membered ring of the dimer anion are relatively loose in the ground state as mentioned above. We therefore conclude that generation of $C_2S_2^-$ proceeds on the ground state PES. The appearance energy of $C_2S_2^-$ may correspond to a dissociation threshold of the ground state anion, unless the internal conversion rate depends significantly on the excitation energy. Thus, the competition between the dissociation channels is attributed to their similar decay rates of the excited state due to direct dissociation and for internal conversion.

IV. CONCLUDING REMARKS

We observed photodestruction spectra of $(CS_2)_n^-$, which show that the clusters are composed of the dimer core anion $C_2S_4^-$ and the surrounding neutral CS_2 molecules. Three competitive destruction channels of the dimer anion were found after the photoexcitation of the dimer anion, $C_2S_4^-$, electron detachment and two dissociation processes. One of the dissociation processes leads to the $C_2S_2^-$ generation, which competes the ordinary dissociation into CS_2^- and CS_2. By using *ab initio* calculations, the most stable geometry of the dimer anion examined is of the form having a four-membered ring involving a C–C bond formation. Such a C–C covalent bond has never been observed in reactions of the neutral and the cationic clusters of CS_2.[6] Thus, we assume that reactivity of anions is important to linear carbon chain formation[29] in discharge-induced reactions involving CS_2.

ACKNOWLEDGMENTS

The authors are grateful to Professor K. Kaya and Dr. A. Nakajima of Keio University for valuable advice on the negative ion source. They thank Professor K. H. Bowen of

Johns Hopkins University for providing them with the photoelectron data. They thank Professor T. Nagata of Tokyo University for stimulating discussions about photoelectron spectra of $(CS_2)_n^-$. Thanks are due to Dr. A. Fujii for his help at the early stage of this work, and also to Professor T. Ebata and Dr. H. Ishikawa for helpful discussions.

[1] S. T. Arnold, J. G. Eaton, D. Patel-Misra, H. W. Sarkas, and K. H. Bowen, in *Ion and Cluster Ion Spectroscopy and Structure*, edited by J. P. Maier (Elsevier, Amsterdam, 1989), p. 417, and references therein.
[2] Y. Hatano, in *Dynamics of Excited Molecules*, edited by K. Kuchitsu (Elsevier, Amsterdam, 1994), p. 151.
[3] J. Tsukamoto and A. Takahashi, Jpn. J. Appl. Phys., Part 2 **25**, L338 (1989).
[4] Y. Asano, Jpn. J. Appl. Phys., Part 1 **22**, 1618 (1983).
[5] Y. Ono, S. H. Linn, H. F. Prest, M. E. Gress, and C. Y. Ng, J. Chem. Phys. **73**, 2523 (1980).
[6] Y. Ono, S. H. Linn, H. F. Prest, M. E. Gress, and C. Y. Ng, J. Chem. Phys. **74**, 1125 (1981).
[7] T. Kondow and K. Mitsuke, J. Chem. Phys. **83**, 2612 (1985).
[8] K. Hiraoka, S. Fujimaki, K. Aruga, and S. Yamabe, J. Phys. Chem. **98**, 1801 (1994).
[9] T. Tsukada, T. Hirose, and T. Nagata, Chem. Phys. Lett. (in press).
[10] S. H. Fleischman and K. D. Jordan, J. Phys. Chem. **91**, 1300 (1987).
[11] M. J. DeLuca, B. Niu, and M. A. Johnson, J. Chem. Phys. **88**, 5857 (1988).
[12] M. L. Alexander, M. A. Johnson, N. E. Levinger, and W. C. Lineberger, Phys. Rev. Lett. **57**, 976 (1986).
[13] T. Maeyama, T. Tsumura, A. Fujii, and N. Mikami, Chem. Phys. Lett. **264**, 292 (1997).
[14] A. Nakajima, T. Taguwa, K. Hoshino, T. Sugioka, T. Naganuma, F. Ono, K. Watanabe, K. Nakao, Y. Konishi, R. Kishi, and K. Kaya Chem. Phys. Lett. **214**, 22 (1993).
[15] P. C. Cosby, R. A. Bennett, J. R. Peterson, and J. T. Moseley, J. Chem. Phys. **63**, 1612 (1975).
[16] J. M. Oakes and G. B. Ellison, Tetrahedron **42**, 6263 (1986).
[17] K. Ohashi and N. Nishi, J. Phys. Chem. **96**, 2931 (1992).
[18] K. Ohashi and N. Nishi, J. Chem. Phys. **98**, 390 (1993).
[19] R. V. Hodges and J. A. Vanderhoff, J. Chem. Phys. **72**, 3517 (1980).
[20] T. Dresch, H. Kramer, Y. Thurner, and R. Weber, Z. Phys. D **18**, 391 (1991).
[21] G. P. Smith and L. C. Lee, J. Chem. Phys. **69**, 5393 (1978).
[22] C. B. Freidhoff, Ph.D. thesis, 1987, Johns Hopkins University; private communication from Professor K. H. Bowen.
[23] T. Dresch, H. Kramer, Y. Thurner, and R. Weber, Chem. Phys. Lett. **177**, 383 (1991).
[24] M. J. Frisch, G. W. Trucks, H. B. Schlegel, P. M. W. Gill, B. G. Johnson, M. W. Wong, J. B. Foresman, M. A. Robb, M. Head-Gordon, E. S. Replogle, R. Gomperts, J. L. Andres, K. Raghavachari, J. S. Blinkley, C. Gonzalez, R. L. Martin, D. J. Fox, D. J. Defrees, J. Baker, J. J. P. Stewart, and J. A. Pople, GAUSSIAN 92/DFT, Rev. G.2, Gaussian Inc., Pittsburgh, PA, 1993.
[25] We also calculated at the BLYP level of theory, where the optimized geometries and energies are remarkably different from those obtained at the HF level. However, application of density functional methods for negative ions is not well established at present; see Ref. 26.
[26] J. M. Galbraith and H. F. Schaefer III, J. Chem. Phys. **105**, 862 (1996).
[27] G. Herzberg, Molecular Spectra and Molecular Structure (Krieger, Malabar, 1989), Vol. 1, p. 566.
[28] G. Herzberg, Molecular Spectra and Molecular Structure (Van Nostrand Reinhold, New York, 1966), Vol. 3, p. 600.
[29] See, for example, Y. Ohshima and Y. Endo, J. Mol. Spectrosc. **153**, 627 (1992).